FULL-LENGTH PAPER

Structure and specificity of an anti-chloramphenicol single domain antibody for detection of amphenicol residues

Charles A. Swofford[1,2] | Sarah A. Nordeen[1] | Lu Chen[2] |
Mahaam M Desai[2] | Joanna Chen[2] | Stacy L. Springs[2] |
Thomas U. Schwartz[1] | Anthony J. Sinskey[1,2]

[1]Department of Biology, Massachusetts Institute of Technology, Cambridge, Massachusetts, USA

[2]Center for Biomedical Innovation, Massachusetts Institute of Technology, Cambridge, Massachusetts, USA

Correspondence
Charles A. Swofford, 77 Massachusetts Ave, BLDG E19-60, Cambridge, MA 02139, USA.
Email: cswoff@mit.edu

Funding information
Walmart Foundation

Review Editor: Aitziber Cortajarena

Abstract

Antibiotics in aquaculture prevent bacterial infection of fish, but their misuse is a public health risk and contributes to the unintentional creation of multiresistant pathogens. Regulatory agencies cannot do the rigorous, expensive testing required to keep up with the volume of seafood shipments. Current rapid test kits for these drugs enable the increase in testing needed for adequate monitoring of food supply chains, but they lack a high degree of accuracy. To combat this, we set out to discover and engineer single-domain antibodies (VHHs) that bind to small molecule antibiotics, and that can be used in rapid test kits. The small size, solubility, and stability of VHHs are useful properties that can improve the reliability and shelf-life of test kits for these adulterants. Here, we report a novel anti-chloramphenicol VHH (Chl-VHH) with a disassociation constant of 57 nM. This was achieved by immunizing a llama against a chloramphenicol-keyhole limpet hemocyanin (KLH) conjugate and screening for high affinity binders through phage display. The crystal structure of the bound-VHH to chloramphenicol was key to identifying a mutation in the binding pocket that resulted in a 16-fold improvement in binding affinity. In addition, the structure provides new insights into VHH-hapten interactions that can guide future engineering of VHHs against additional targets.

KEYWORDS
antibiotics, chloramphenicol, food adulteration, haptens, nanobodies, single-domain antibodies, VHH

1 | INTRODUCTION

Seafood is one of the largest traded commodities in the world today and over half originates in developing countries.[1] In 2019, the United States imported over 6.2 billion pounds of seafood, the majority originating from Chinese aquaculture operations.[2] Due to the high rates of bacterial infection, antibiotics or chemicals such as malachite green, nitrofurans, and fluoroquinolones are often introduced into aquaculture areas to increase the survival rates of fish, but the drug residues can remain through harvesting, processing, and consumption.[3] Moreover,

prolonged exposure to these compounds have been shown to have a carcinogenic effect.[4] The presence of these drug residues also contributes to an increase of antimicrobial resistance (AMR) in human pathogens. For example, the colistin resistance gene MCR-1 was first reported in China in 2015 and soon spread to over 50 countries, including the first reported case in the US in 2016.[5,6] A recent study has shown that a ban on the use of colistin in food animals led to a substantial decline in colistin resistance in both animals and humans in China, highlighting the necessity and effectiveness for timely interventions to address AMR risks at the source.[7]

In 2015, the FDA examined 2.2% of all imported seafood entry lines for a variety of food safety issues. Based on this level of testing, seafood shipments from a foreign processing facility would have a roughly 1 in 1,000 chance of being selected by FDA for drug residue testing, meaning that much of the imported unsafe seafood enters the US supply chain undetected.[1] One of the major reasons that inspection agencies cannot increase the volume and frequency of safety tests is both the cost and time required to do the rigorous analytical experiments using HPLC and mass spectrometry to determine all the potential adulterants in a food product. Very few methods that can detect a broad range of antibiotics exist,[8–10] due to the difficulty in the extraction of compounds with different physicochemical properties.[11] Current rapid test kits for these adulterants, such as immunoassays or biosensors, usually require a biological sensing component that loses its activity in hours or days due to environmental stresses such as pH, temperature, or ionic strength.[12] Rapid tests increase the throughput required to for adequate monitoring of food supply chains, but generally have low accuracy.

Antibodies have long been used in diagnostic and therapeutic applications as highly selective binders to a target of interest, but their large size and multiple domains make library screening difficult and limit their binding capabilities in challenging environments such as high temperatures or after long-term storage.[13] The discovery of heavy chain-only antibodies (VHH IgG) in camelids, however, spawned a promising new field of antibody engineering, since they can be minimized into a single variable domain called a nanobody or VHH. The small size of VHHs provides many favorable properties for biotechnological applications. VHHs can be recombinantly expressed in *E. coli* to ease library screening and allow for functionalization, show excellent solubility compared to conventional antibodies, and are resistant to elevated temperatures and chemical denaturation.[14] Previous studies have shown that VHHs can be stored at 4°C and can tolerate incubation at 37°C for several months,

indicating an improved shelf life for a diagnostic platform.[15] These useful properties indicate that if coupled to a sensor, VHHs might be ideal selective binders for a target of interest in a complicated environment such as food.

While VHHs have been engineered to bind to large molecules such as proteins, less work to date has been done to develop VHHs against small molecules. Previous studies have isolated VHHs against diverse small molecules, such as mycotoxins, insecticides, biomarkers, and flame retardants.[16–22] The affinities are not consistently high, therefore technological applications are still rare. Here, we immunized a llama (*llama glama*) for VHHs against two antibiotics and one antibiotic residue commonly implicated in food supply chain adulteration: chloramphenicol, enrofloxacin, and semicarbazide. We discovered VHHs that bind to chloramphenicol by phage display and quantified their binding affinities through ELISA and isothermal calorimetry (ITC). The crystal structure bound to chloramphenicol was solved and used to improve the affinity of the VHH to chloramphenicol through rational design. This is the first reported anti-chloramphenicol VHH and provides a robust recognition element for the development of biosensors for chloramphenicol detection in food and water products.
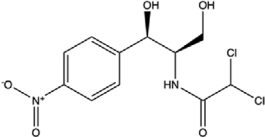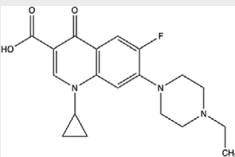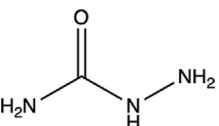
2 | RESULTS

2.1 | Llama immunization

A llama (*Lama glama*) was immunized against a cocktail of three different small molecules,[1] chloramphenicol,[2] enrofloxacin, and[3] semicarbazide, each conjugated to Keyhole Limpet Hemocyanin (KLH), a carrier protein used to illicit immune responses with haptens. These molecules were chosen based on their prevalence in Chinese food supply chains, their varying structures, and their different mechanisms of action (Table 1). Chloramphenicol and enrofloxacin are both veterinary antibiotics that are commonly detected in food products but are banned by the China Food and Drug Administration (CFDA).[23] Semicarbazide, on the other hand, is a metabolic marker of the banned antimicrobial, nitrofurazone, and is the common analyte used for detecting nitrofurazone adulteration.[24]

After three injections of the cocktail containing 500 μg of each antibiotic-carrier protein conjugate, the llama exhibited a 199-fold response to a chloramphenicol-OVA conjugate using an ELISA titration assay of the serum after 50 days compared to the day 1 control (Table 1; Supplemental Figure 1). Enrofloxacin-

TABLE 1 Small Molecules Chosen for Llama Immunization

Antibiotic	Size (MW)	Mechanism of action	Implication in food safety (Li et al.)	Llama titer after 50 days (1: x serum dilution with response to OVA-antibiotic conjugate)	Fold increase in titer compared to day 1 control
Chloramphenicol	323.13	Inhibits protein synthesis by binding to the active site of bacterial ribosomes	Implicated in 17% of Chinese food fraud identified by a national food safety inspection	52,100	199
Enrofloxacin	359.4	Interferes with DNA replication by inhibiting ligase activity of topoisomerases and gyrases	Enrofloxacin and ciprofloxacin (metabolic derivative) implicated in 12% of Chinese food fraud identified by a national food safety inspection	2,370	8.8
Semicarbazide	75.08	Detectable metabolite of nitrofurazone, an antibiotic that inhibits DNA synthesis	Antibiotic precursor nitrofurazone implicated in 10% of Chinese food fraud identified by a national food safety inspection	299	299

OVA exhibited a weaker 8.8-fold response. Semicarbazide-OVA showed a strong response compared to the day 1 control, however, the overall response was much lower than the other two after Day 50, with the serum only diluted 300-fold before signal was lost on the ELISA assay. For comparison, the serum had to be diluted over 52,000-fold before signal was lost against chloramphenicol, suggesting that VHHs against this target was most likely upregulated. To maximize the probability that an VHH could be isolated against one of these targets, chloramphenicol was used for all subsequent experiments.

2.2 | Panning strategy comparison

Unlike traditional phage display against a protein, isolating an VHH against chloramphenicol presents a unique challenge, as it is difficult to immobilize a small molecule during the wash steps necessary to remove unbound phage. To solve this problem, we adapted three different panning strategies developed by Pirez-Schirmer et al.[25]: selective competition, simultaneous competition, and off-rate selection (Figure 1a). In all three strategies,

chloramphenicol is covalently attached to BSA and coated to the surface of a 96-well plate. The BSA-small molecule conjugate is then probed against the phage library and unbound phage is washed away. At this point, the challenge is to select for VHHs that bind specifically to chloramphenicol, and not the BSA-chloramphenicol conjugate. To select for only the chloramphenicol, the strategies are outlined as follows:

1. Selective competition mixes chloramphenicol in the well with the bound phage and aims to remove phage that preferentially binds to the small molecule over the BSA-chloramphenicol conjugate.
2. Simultaneous competition lyses all bound phage, mixes the phage with chloramphenicol alone in a tube, and then reintroduces the phage to a new well plate with the BSA-chloramphenicol conjugate coated to the plate. Any phage that binds to the chloramphenicol will have its active site blocked and can be removed in the eluate after an incubation period.
3. Off-rate selection mixes chloramphenicol in the well plate with bound phage and then washes off phage that bind only to the small molecule. The remaining binders to the plate are then removed by trypsin. The
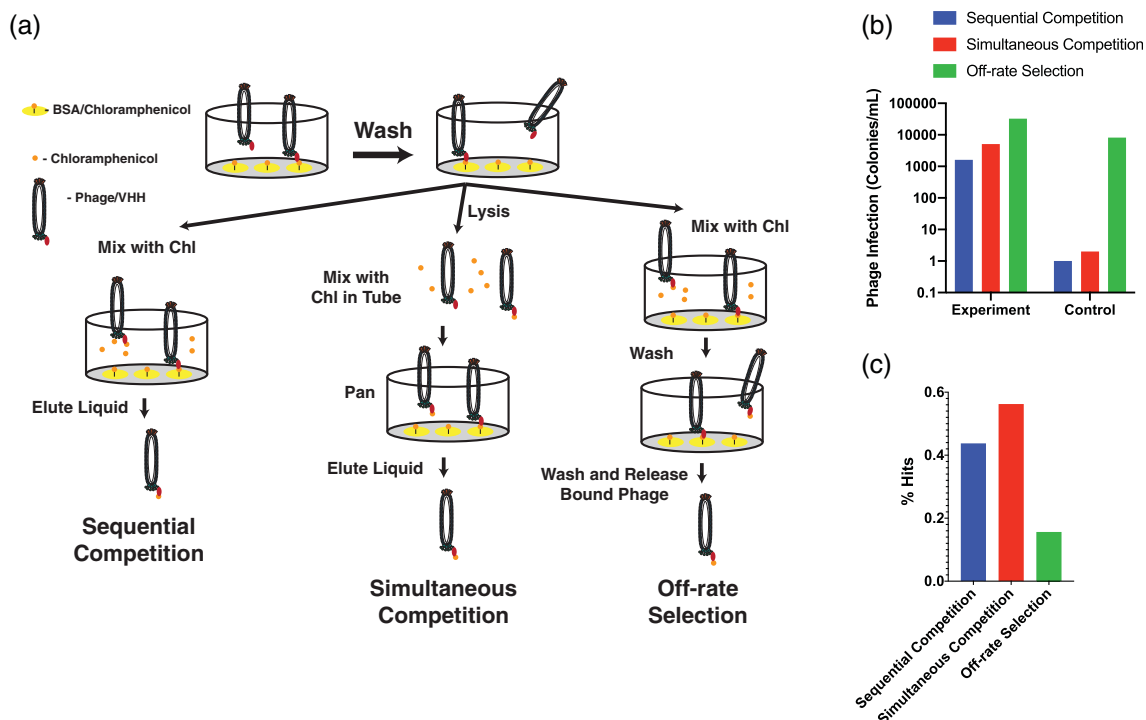
FIGURE 1 Panning strategies and results for chloramphenicol-specific VHH isolation. (a) Three panning strategies were adapted from Pírez-Schirmer et al. for the isolation of VHHs with high specificity to chloramphenicol. In all strategies, the phage library is initially panned against immobilized BSA-chloramphenicol and unbound phage is removed in the wash steps. Sequential competition mixes the hapten in the well with the bound phage and aims to remove phage that preferentially binds to the hapten over the BSA-hapten conjugate. Simultaneous competition lyses all bound phage, mixes the phage with the hapten alone in a tube, and then reintroduces the phage to a new well plate with the BSA-hapten conjugate coated to the plate. Any phage that binds to the small molecule will have their active site blocked and can be removed in the eluate after an incubation period. Off-rate selection mixes the hapten in the well plate with bound phage and then washes off phage that bind only to the hapten. The remaining binders to the plate are then removed by trypsin digestion. b) Number of phage-infected *E. coli* colonies after each panning procedure. The control experiment involved panning against unconjugated BSA coated to the well. c) Percent of colonies that secreted a VHH with specificity to BSA-chloramphenicol in an indirect ELISA, based on panning procedure

idea of this selection is that strong binders will always remain bound to the BSA-chloramphenicol conjugate and the weak binders will be removed.

After each strategy is complete, remaining phage is transfected into *Escherichia coli* ER2738 and isolates are selected based on a carbenicillin resistance cassette carried by the phage.

For each strategy, the number of carbenicillin-resistant colonies were counted after transfection to assess how many phages were bound after each panning procedure. This number was compared to a control involving panning against unconjugated BSA coated to the wells. The results confirmed that all three strategies can isolate phages against chloramphenicol, although sequential and simultaneous competition were much better at removing phage with non-specific binding compared to off-rate selection (Figure 1b). For sequential and simultaneous competition, there we one and two colonies

per ml of culture, respectively, that grew on the control panning experiment. Off-rate selection had the greatest number of colonies in both the experimental and control groups, but only a four-fold increase in colonies for the experimental group as compared to the control.

After panning, 32 *E. coli* isolates from each strategy were induced with IPTG to secret VHHs and the supernatant was assessed on an indirect ELISA against a chloramphenicol-BSA conjugate. Sequential (43%) and simultaneous competition (56%) both had a higher percentage of positive hits in the ELISA compared to 16% for off-rate selection (Figure 1c). This was expected, as off-rate selection clearly had a higher background of non-specific phage, as evidenced by the high number of colonies after selection in the control group (Figure 1b). Despite this, three out of the top 10 hits as assessed by replicate ELISAs came from off-rate selection (Supplemental Figure 2), suggesting that while background is higher, many strong binders can also be found
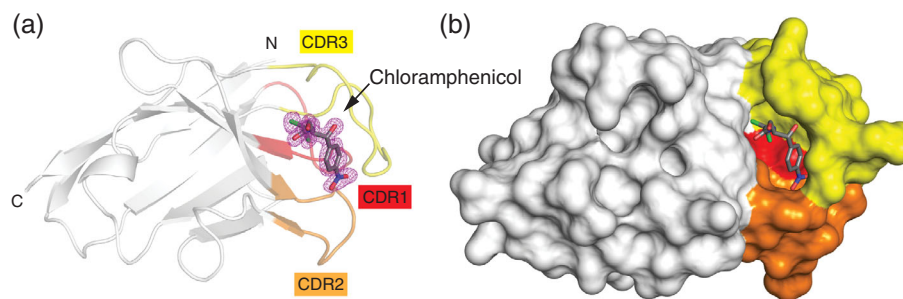
FIGURE 2 Crystal structure of VHH Chl-B2. (a) Cartoon representation of VHH Chl-B2. Bound chloramphenicol in ball-and-stick, with $2F_o–F_c$ density contoured at 1.5σ around the ligand. CDR1-3 are colored in red, orange, and yellow, respectively. (b) Surface representation of the complex in the same orientation as in (A). Chloramphenicol occupies a deep binding pocket grafted primarily by the three CDRs

FIGURE 3 Close-up view of the VHH Chl-B2/F47W ligand interaction. (a) Details of the interaction between chloramphenicol (grey) with VHH Chl-B2. Color scheme as in Figure 3. Note the single hydrogen-bond between a hydroxyl group of chloramphenicol and the backbone carbonyl of R109. (b) Same as in (A), except for modeling a tryptophane in place of phenylalanine in position 47. Increased chloramphenicol affinity of Chl-B2 (F47W) (Chl-VHH) compared to Chl-B2 suggests the formation of a new hydrogen-bond between the ligand and the VHH
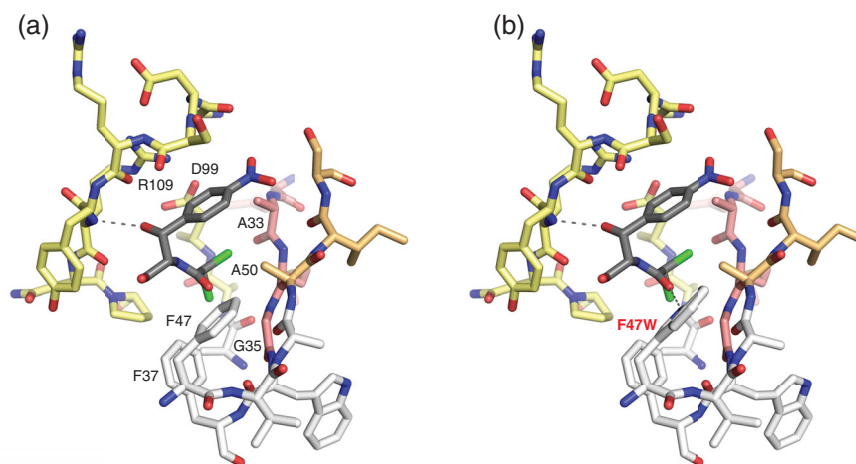
using this method. Based on the ELISA screen from all three panning strategies (Supplemental Figure 2), we sequenced the top 10 binders. A comparison of these sequences revealed seven unique sequences from these 10 hits (Supplemental Table 2) and a highly conserved consensus sequence with 86% sequence identity (Supplemental Figure 3). A 6xHis-tag was attached to the top two chloramphenicol binders (Chl-B2 and Chl-D1) from all three panning strategies (Supplemental Figure 2) and purified using immobilized metal affinity chromatography (IMAC) for further analyses.

2.3 | Crystal structure of Chl-B2 bound to chloramphenicol

Since both Chl-B2 and Chl-D1 have 89% homology in their respective amino acid sequences, we aimed to solve their crystal structures to understand which residues play a role in chloramphenicol-binding (Figure 2, PDB Code 7TJC). We were able to obtain crystals of Chl-B2 bound to chloramphenicol and solved the complex structure at a 1.35 Å resolution (Figure 2a). The three CDRs of the

VHH together generate a tight binding pocket for the chloramphenicol ligand with a 325 Å^2 binding surface. CDR1 and CDR2 form the floor of the pocket, while the CDR3 folds into a lid that traps the ligand (Figure 2b). Characteristically short residues, alanine 33, glycine 35, and alanine 50 sculpt the pocket floor. CDR3 loops over the binding pocket and is held in place by aspartate 99 and arginine 109 forming a salt bridge (Figure 3a). It is primarily backbone contacts, include one single hydrogen bond, that coordinate the ligand through CDR3. The exquisite surface complementarity of the pocket is illustrated by the fact that no water molecule is used to fill gaps, as it is often the case for less tightly bound, rather hydrophilic ligands.

The paucity of hydrogen bonds led us to consider point mutations that may add additional hydrogen bonds, thereby possibly increasing affinity. We noticed that modeling phenylalanine 47 as tryptophan, as it is in Chl-D1, would enable a second hydrogen bond between the carbonyl of the amide bond in the ligand and the indole nitrogen (Figure 3b, Supplemental Figure 4). Thus, we set out to characterize the binding behavior of the mutant.
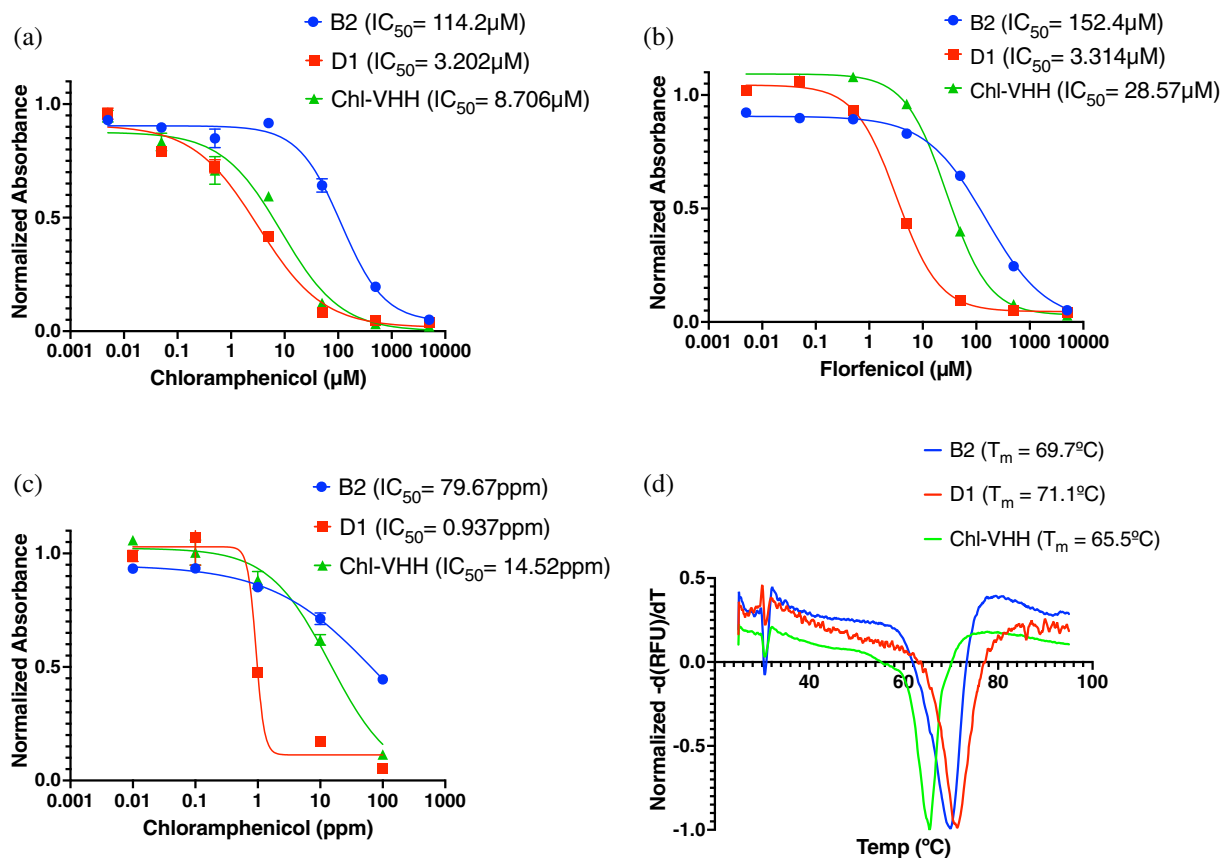
FIGURE 4 Competitive ELISAs and thermal stability of chloramphenicol-specific VHHs. (a) Competitive ELISA of three VHHs against chloramphenicol. (b) Competitive ELISA of three VHHs against florfenicol. (c) Competitive ELISA of three VHHs against chloramphenicol extracted from a tilapia extract. For all ELISA experiments, 500pM of each nanobody was incubated with different concentrations of the sample for 1 hr and then added to a plate coated with 50 ng of BSA-chloramphenicol. A Rabbit anti-His secondary conjugated with HRP was used for detection. Normalized absorbance is calculated as the fraction of absorbance relative to a negative control with no antibiotic. Error bars represent SEM from triplicate wells. (d) Thermal stability of three VHHs using a GloMelt™ Thermal Shift Stability Kit. The y-axis represents the first derivative (slope) of the fluorescence with respect to temperature. Fluorescence was normalized as a fraction of the maximum value over the course of the experiment. The melting temperature is determined by the temperature at which the first derivative of the fluorescence reaches a minimum

2.4 | Indirect and competitive ELISAs indicate VHH binding to chloramphenicol

The F47W mutation was introduced in the expression plasmid for Chl-B2 to purify a new VHH, Chl-VHH. In an indirect ELISA against 50 ng of BSA-chloramphenicol, Chl-VHH had an IC_{50} concentration of 0.02 nM, the lowest of the three VHHs tested (Supplemental Figure 5). This was a five-fold improvement over Chl-B2 and a 10-fold improvement over Chl-D1. A competitive ELISA was then used to determine if the VHHs could bind to chloramphenicol in solution. For all competitive ELISA experiments, 0.5 nM of VHH was used for incubation, since this concentration was above the IC_{50} value determined in the indirect ELISA and would ensure an absorbance signal in the negative control (Supplemental Figure 5). VHHs was incubated with chloramphenicol for 1 hr and then the mixture was added to a plate coated with 50 ng of BSA-chloramphenicol. Chl-D1 had the lowest IC_{50} concentration of 3.202 μM, a 2.7- and 36-fold improvement over Chl-VHH and Chl-B2 respectively (Figure 4a). By introducing the F47W mutation into Chl-B2, the IC_{50} concentration improved 13-fold.

We used the same competitive ELISA to evaluate the VHHs binding affinity to florfenicol, a closely related analog to chloramphenicol (Figure 4b). Once again, Chl-D1 had the lowest IC_{50} concentration of 3.3 μM, a 2.7- and 46-fold improvement over Chl-VHH and Chl-B2 respectively. Chl-VHH and Chl-B2 had moderate preferential binding to chloramphenicol based on IC_{50} concentration (3.2-fold and 1.3-fold respectively), but Chl-D1 bound equally to both molecules.
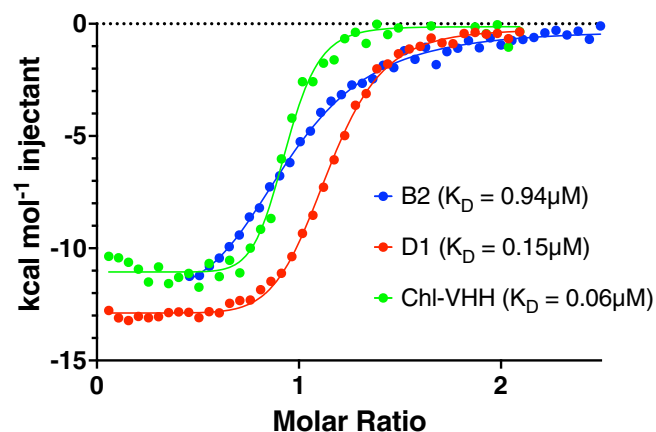
FIGURE 5 Binding affinities of VHHs against chloramphenicol. Enthalpy per mole of chloramphenicol injected vs. the molar ratio of chloramphenicol to each single-domain antibody in the reaction chamber

2.5 | Evaluation of chloramphenicol-specific VHHs for ELISA test-kits

In order to test the VHHs in a complex matrix, chloramphenicol was spiked at various concentrations in 3 g of homogenized tilapia and extracted following the procedure outlined in a commercially available chloramphenicol ELISA kit (PerkinElmer). Fish extracts were used in the competitive chloramphenicol ELISA outlined earlier. Chl-D1 had the highest binding affinity to chloramphenicol (IC_{50} = 0.937 ppm) and an 85- and 15-fold improvement over Chl-B2 and Chl-VHH, respectively (Figure 4c). Based on the 6 ml of ethyl acetate used for the initial extraction, the binding affinity of Chl-D1 corresponds to an IC_{50} concentration of 1.55 μM, which is the same order of magnitude seen on the pure chloramphenicol sample tests (Figure 4a). This demonstrates that all three VHHs can detect chloramphenicol in complicated matrices such as fish extracts.

The thermal stability of each VHH was determined using a GloMelt™ protein kit to determine if the VHHs could operate under a variety of temperatures. All three VHHs had melting temperatures (T_M) over 65°C, with Chl-D1 having the highest T_M of 71.1°C (Figure 4d). The F47W mutation in Chl-VHH reduced the T_M from 69.7 to 65.5°C. Chl-D1 also contains this mutation, suggesting that additional mutations in Chl-D1 confers additional stability.

2.6 | Isothermal calorimetry confirms improved binding with key mutation

While competitive ELISAs are helpful for determining VHH binding affinities, they are inherently an indirect measurement of binding since the assay is dependent on the respective affinities of the VHH to the hapten-protein conjugate vs. the hapten itself. Isothermal titration calorimetry (ITC) was used to determine the direct binding affinities of Chl-B2, Chl-D1, Chl-VHH, as well as other relevant thermodynamic parameters such as the enthalpic and entropic changes upon binding (Figure 5, Table 2). As evidenced by the earlier ELISA data (Figure 4), Chl-D1 had the highest affinity for chloramphenicol compared to Chl-B2 and Chl-VHH. The ITC results, on the other hand, indicate that Chl-VHH (K_D = 60 nM) has a 2.5-fold increase in binding affinity to chloramphenicol compared to Chl-D1 (K_D = 150 nM) and a 1.8-fold increase to florfenicol (Table 2). In addition, by introducing the F47W mutation in Chl-B2 (Chl-VHH), the binding affinity was improved 16-fold against chloramphenicol and three-fold against florfenicol. All three VHHs bound poorly to thiamphenicol, another chloramphenicol analog implicated in antibiotic adulteration.

The ITC results were also used to calculate additional thermodynamic parameters and determine the enthalpic (ΔH) and entropic ($-T\Delta S$) contributions to the overall free energy change (ΔG). For all three VHHs, the binding is dominated by a favorable binding enthalpy and a smaller unfavorable binding entropy at room temperature (Table 2). When the F47W mutation was introduced into Chl-B2, the unfavorable entropic contribution was improved 1.87-fold, although this was partially offset by a 1.25-fold reduction in the enthalpic contribution.

3 | DISCUSSION

Here, we describe a single-domain antibodies capable of binding to chloramphenicol, one of the most common antibiotic adulterants found in Asian food supply chains, despite being banned by both the Chinese and US FDA. By immunizing a llama against chloramphenicol conjugated to a carrier protein, we were able to isolate VHHs with specificity to chloramphenicol, as well as its amphenicol analogues. Using X-ray crystallography to visualize the binding pocket, a point mutation was made to improve the VHH binding affinity and level of detection for downstream applications. Because this VHH can be expressed in *E. coli*, it can be mass produced for use with rapid antigen-based testing kits at low cost for field testing throughout a supply chain.

Although many hapten-VHH conjugates have been discovered, few structures have been published in the PDB that can help guide library screening for small molecule selectivity. To date, structures have been published for two azo-dyes Reactive Red 6 (RR6)[26] and Reactive

TABLE 2 Thermodynamic parameters of each VHH in response to chloramphenicol analogs

	Chloramphenicol			Florfenicol			Thiamphenicol		
	B2	D1	Chl-VHH	B2	D1	Chl-VHH	B2	D1	Chl-VHH
Kd (μM)	0.94	0.15	0.06	1.10	0.58	0.33	5.26	2.25	3.03
ΔG (x10^3 kcal/mol)	−8.2	−9.3	−9.9	−8.1	−8.5	−8.8	−7.2	−7.7	−7.5
ΔH (x10^4 kcal/mol)	−2.0	−1.9	−1.6	−2.0	−2.4	−1.6	−2.1	−2.9	−2.2
$-T\Delta S$ (x10^3 kcal/mol)	12	9.9	6.4	12	16	6.7	−4.8	21	14

Red 1 (RR1),[27] methotrexate (MTX),[28] triclocarban (TCC),[29] cortisol,[30] and a homodimer VHH that binds to caffeine.[31] The VHH-chloramphenicol interaction was sterically most like the VHH-RR1 binding motif (PDB Code 1I3U). In both cases, the long CDR3 loop played an important role in trapping the ligand by folding into a lid over the CDR1 and CDR2 floor of the pocket (Figure 2, Supplemental Figure 6A,B). On the other hand, most VHH-hapten crystal structures such as MTX (454.44 Da), TCC (315.58 Da), and cortisol (362.46 Da, Supplemental Figure 6C) reveal a different binding motif: the haptens have limited interactions with CDR3 and instead, the hydrophobic core of the haptens inserts into the under-loop tunnel formed by CDR1.[30] These data suggest that not all VHHs develop a CDR1 tunneling mode to bind small molecular weight hydrophobic haptens and screening a diverse CDR3 library will also be useful in future VHH-hapten discovery.

When comparing the reported binding affinity for different small molecules bound to VHHs, there exists a wide range from low nanomolar (RR1, RR6)[26,27] to medium micromolar (cortisol).[30] The difference in binding surface between these small molecules is not dramatic, but there is a strong correlation between the number of hydrogen-bonds and the binding strength. For example, RR1 binds its cognate VHH via 8 hydrogen bonds with 22 nM affinity,[27] while cortisol, on the other end of the spectrum, exhibits no hydrogen bonds and a $\sim$ 20 μM affinity.[30] This was the main rationale for us to try to improve binding affinity via adding hydrogen bonds. Mutations in the constant region of the VHH can also increase affinity to haptens by adding novel binding sites. For example, the anti-MTX VHH affinity was improved 1,000-fold by mutating sites along a "CDR4" nonhypervariable loop that came into contact with the hapten.[28] This is the only example to date of a VHH structure being used to successfully improve binding affinity. Here, the binding affinity of Chl-B2 was improved by mutating a key amino acid (F47W) in the constant region to form a new hydrogen-bond with the hapten (Figure 3).

Despite discovering a VHH with moderate affinity for chloramphenicol, the phage library did not yield hits for enrofloxacin or semicarbazide. The low titer response of the llama serum to enrofloxacin and semicarbazide suggested that discovering VHHs against these targets would prove difficult (Supplemental Figure 1). Unlike conventional antibodies, VHHs lack the heavy/light chain interface that typically forms the binding pocket that can accommodate haptens, making them more difficult to discover and isolate through immune libraries.[28] In addition, hapten design is critically important since presentation of the hapten on a carrier protein can greatly affect its immunogenicity.[32] Laboratories must also overcome a significant cost and time barrier to run an immunization protocol. To combat this, synthetic VHH libraries for both phage[33] and yeast display[34] have been generated that have successfully been used to discover binders against protein targets. These libraries have not been tested against hapten targets but could be a useful cost-effective tool for small molecules that do not illicit immune responses or require extensive effort to determine the proper presentation on a carrier protein.

Anti-hapten VHHs have been used to detect small molecules in a variety of commonly used formats,[32] including ELISAs,[35,36] surface-plasma resonance (SPR),[16,29,35,36] and lateral flow assays.[37] While binding affinities are important, the design of the assay and the sensing modality can play an important role in the level of detection. For example, Chl-VHH had a 2.5-fold improved affinity to chloramphenicol compared to Chl-D1 using ITC (Table 2), but Chl-D1 consistently outperformed Chl-VHH in ELISAs (Figure 4). This is most likely due to the 20-fold decrease in the IC$_{50}$ of Chl-VHH for the hapten-carrier protein conjugate compared to Chl-D1 (Supplemental Figure 5). To take advantage of Chl-VHH improved affinity, a label-free modality may be required for improved detection. New inexpensive electrochemical methods have been developed that can provide sensitive, label-free detection of a small-molecule to its protein receptor using impedance spectroscopy. For example, an impedance platform was engineered to detect nanomolar levels of estradiol using the native estrogen receptor as a recognition element.[38] These methods could easily be adapted for rapid detection of chloramphenicol, a similar size compound to estradiol,

using Chl-VHH as a recognition element. Coupling Chl-VHH to quantitative, low-cost sensing modalities will provide a deployable technology that can be used to detect chloramphenicol adulterants quickly in food supply chains and could be expanded to other adulterants as further anti-hapten VHH discovery continues.

4 | MATERIALS AND METHODS

4.1 | Immunization

Llama immunization, buffy coat isolation, and RNA purification was completed under a custom contract with Lampire Biological Laboratories (Pipersville, PA). The 500 μg each of Chloramphenicol-Keyhole limpet hemocyanin (KLH) (AAT Bioquest, Sunnyvale, CA), Enrofloxacin-KLH (Creative Diagnostics, Shirley, NY), and Semicarbazide-KLH (AAT Bioquest) was emulsified with Complete Freund's Adjuvant (CFA) in a 1:1 ratio. The 300 μg was then injected intramuscular (IM) at the prescapular nodes, and 200 μg was injected intradermal (ID) at four different sites. At day 21, the injections were repeated as before, although the antigens were emulsified with Incomplete Freund's Adjuvant (IFA) in a 1:1 ratio. At day 30, a test bleed was conducted for an ELISA titration assay to determine the llama response to the three antigens and was used to inform subsequent injection dosage. At day 42, based on the ELISA titration assay results, 750 μg of each antigen was emulsified with IFA at a 1:1 ratio and injected IM only. Finally, at day 50, a production bleed was conducted and used for buffy coat extraction and RNA isolation. A portion of each bleed was also used to determine final titers on an ELISA titration assay (Supplemental Figure 1).

The ELISA titration assay was run in-house at Lampire Biological Laboratories. For each antigen, a 96-well plate was coated with either Chloramphenicol-Ovalbumin (OVA) (AAT Bioquest), Enrofloxacin-OVA (Fitzgerald Industries, Acton, MA), or Semicarbazide-OVA (Cloud-Clone Corp., Katy, TX) and serial dilutions of the llama serum was added to the plates. The ELISA data was fitted to a Four Parameter Logistic (4PL) Regression to determine the point of inflection in the sigmoidal curve that is used to report llama titer (Supplemental Figure 1).

4.2 | Library construction

Three micrograms of purified RNA received from Lampire Biological Laboratories was reverse transcribed using the Superscript III First-Strand Synthesis System (ThermoFisher, Waltham, MA) following manufacturer's instructions. One third of the RNA was reverse transcribed with random hexamers provided by the kit, one third was reverse transcribed with oligo dT provided by the kit, and one third was reverse transcribed using gene-specific primers Al.CH2 and Al.CH2.2 (All primer sequences can be found in Supplemental Table 1). Each of these cDNA fractions was then used to amplify the VHH genes using AlVHH-F1 as a forward primer and either the reverse primer Al-VHH-shR1 for the short hinge VHHs and Al-VHH-lhR1 for the long-hinge VHHs using the HotStarTaq DNA Polymerase (Qiagen, Germantown, MD). The ∼400 bp PCR products were then gel-purified and cloned into the phagemid pD, a generous gift from the Ploegh lab (Boston Children's Hospital, Boston, MA), using the NotI and AscI restrictions sites introduced by the primers. pD has been designed to express phage-displayed recombinant VHHs or soluble VHHs with a C-terminal E-tag, based on the host cells used. The phagemid contains an amber stop codon between the VHH gene and the gene 3 of M13 phage. All restriction enzymes and reagents were purchased at New England Biolabs (Ipswich, MA). The ligated vectors were then transformed into electrocompetent *E. coli* TG1 (Agilent, Santa Clara, CA) and plated on $2 \times$ YT plates supplemented with 2% glucose and 100 μg/ml carbenicillin. TG1 cells produces a suppressor tRNA that allows readthrough of the amber stop codon on pD and produces VHH-displayed phage particles. Transformants were pooled into SOC media containing carbenicillin and 15% glycerol, aliquoted, and stored at $-80°$C to generate the constructed library.

Phage particles were induced by growing a 1 ml of thawed library stock in 100 ml SOC media with 100 μg/ml carbenicillin to an $OD_{600} = 0.5$–0.7 at 37°C. The culture was then infected with 10^{13} pfu of VCMS13 helper phage (gift from the Ploegh lab), grown for 30 min at 37°C without shaking, and then a further 1 hr and 30 min at 37°C with shaking. The culture was then pelleted and resuspended in 100 ml of 2YT media supplemented with 0.1% glucose, 100 μg/ml carbenicillin, and 70 μg/ml kanamycin, then grown overnight at 30°C. Carbenicillin was added for plasmid selection and kanamycin for helper phage selection. The next day, the supernatant was removed, and phage particles were precipitated using a 20% (w/v) Polyethylene glycol (PEG) 8,000/2.5 M NaCl solution, pelleted, washed in the same solution, pelleted again, and resuspended in 1 ml of phosphate-buffered saline (PBS) to generate the phage library for panning.

4.3 | Panning procedure for chloramphenicol

Three panning strategies to isolate phage that bound specifically to chloramphenicol (sequential competition,

simultaneous competition, and off-rate selection) were followed as described previously.[25] For each strategy, *E. coli* infections were performed using the same method. The 500 μl of an overnight culture of *E. coli* ER2738 cells (Ploegh lab) was added to each tube containing eluted phage and incubated for 15 min at 37°C and then plated on 2 × YT medium containing 2% glucose, 10 μg/ml tetracycline, and 100 μg/ml carbenicillin. ER2738 is a non-suppressor strain and recognizes the amber stop codon in pD, meaning that soluble VHHs will be produced upon induction. A small subset of the infected culture was used to create serial dilutions used for determining titers while the remaining portions were plated on larger plates directly. Colonies on the titer plates were counted and used to calculate infection rates.

4.4 | VHH screen

Individual colonies were picked from the panning plates and grown overnight with agitation at 37°C in a 96-well plate using 200 μl of SOC per well, supplemented with 10 μg/ml tetracycline and 100 μg/ml carbenicillin. The next day, 2 μl of each well was used to seed a 180 μl culture of 2YT with 10 μg/ml tetracycline and 100 μg/ml carbenicillin on a new 96-well plate. This new culture was grown for 4 hr at 37°C, induced with 80 μl of 10 mM IPTG, and then grown overnight at 30°C. Meanwhile, a separate ELISA plate was coated with 0.5 μg/ml Chl-BSA in PBS overnight at 4°C.

The next day, the wells of the ELISA plate were blocked with 200 μl of 5% milk and 0.05% Tween-20 in PBS for 2 hr at room temperature. Afterwards, 50 μl of supernatant from the culture plate was added to the ELISA plate, along with 50 μl of blocking buffer and incubated for 1 hr at room temperature. The ELISA plate was then washed six times with PBST and 100 μl of Goat anti-E-tag conjugated to horseradish peroxidase (HRP) (Abcam, Cambridge, MA) diluted 1:10,000 was added to each well. After another one-hour incubation at room temperature and six subsequent washes with PBST, 100 μl of 1-step™ TMB solution (ThermoFisher) was added to each well and the reaction was stopped with 100 μl of 1 N HCl. Finally, the plate was analyzed in a Varioskan plate reader (ThermoFisher) at an absorbance of 450 nm to assess binding.

4.5 | VHH purification

VHHs that were deemed strong binders in the ELISA screen were cloned into the periplasmic expression vector pHEN6, a generous gift from the Ploegh lab, using

Gibson assembly and the primers described in Supplemental Table 1. All VHHs were then purified using IMAC as described previously.[39]

4.6 | Competitive ELISAs

Purified VHHs were first tested on routine indirect ELISAs using the procedure outlined earlier for the initial screen. The only changes to the earlier protocol were that purified VHHs were added as a primary at various concentrations and a Rabbit anti-6xHis-tag antibody conjugated to HRP (Abcam) was used as a secondary. For the competitive ELISA, various concentrations of chloramphenicol were mixed for 1 hr with 0.5 nM of purified VHH before being added to a plate coated with 500 ng/ml of BSA-chloramphenicol. The Rabbit anti-6xHis-tag antibody conjugated to HRP was also used as a secondary for these experiments. The ELISA data was fitted to a Four Parameter Logistic (4PL) Regression to determine the point of inflection in the sigmoidal curve that is used to report IC_{50} concentration.

4.7 | Chloramphenicol extraction from seafood

The protocol for extracting chloramphenicol from seafood was adapted from the MaxSignal® Chloramphenicol ELISA Kit (PerkinElmer, Waltham, MA). Briefly, a filet of store-bought Tilapia sourced from China was homogenized in a Magic Bullet compact blender. Three grams of fish were spiked with various concentrations of chloramphenicol in 6 ml of ethyl acetate. Extraction was then followed according to the manufacturer's instructions. Fifty microliters of the sample extract were mixed with 50 μl of 1 nM of purified VHH (for a final concentration of 0.5 nM) before being added to a plate coated with 500 ng/ml of BSA-chloramphenicol. The competitive ELISA was then carried out as outlined earlier.

4.8 | Thermal stability assay

The GloMelt™ Thermal Shift Stability Kit (Biotium Inc., Freemont, CA) was used to determine the melting temperature of each VHH.0.5 μg/μl was used for each protein and protocol was followed according to manufacturer's instructions. The minimum of the first derivative of fluorescence with respect to temperature was used to determine the melting temperature for each VHH.

4.9 | Isothermal calorimetry to determine thermodynamic binding parameters

For isothermal calorimetry, the VHH was buffer exchanged into fresh PBS using a 10 K MWCO Slide-a-lyzer dialysis cassette (Thermo) and then diluted to a concentration of 1 μM. A MicroCal VP-ITC (Malvern Panalytical, Westborough, MA) was used for running the experiment and 1.4 nmol of VHH was added to the reaction number. For each antibiotic tested, it was first dissolved in the same PBS used for the VHH and diluted appropriately. Afterwards, 2.8 nmol of the antibiotic was loaded into the syringe and 5 μl was injected into the chamber every 4 min for 40 total injections. Thermodynamic parameters were calculated from the thermograms using the Origin analysis software (Malvern Panalytical).

4.10 | Crystallization

Chl-B2 was concentrated to 13.3 mg/ml and subsequently diluted with freshly made 5 mM chloramphenicol (Calbiochem) in gel filtration buffer to a final concentration of 10 mg/ml Chl-B2 and 1.25 mM chloramphenicol. Crystals of Chl-B2 + chloramphenicol were obtained at 18°C in 2 days as part of the JCSG+ suite (Qiagen) in a 96-well sitting drop tray with a reservoir containing 0.1 M sodium acetate pH 4.5 and 1 M ammonium hydrogen phosphate. The rod-shaped crystals continued to grow over the next 20 days. Crystals were transferred into a cryo-protectant solution containing the crystallization condition with 15% glycerol and 1.25 mM chloramphenicol and cryo-cooled in liquid nitrogen. Crystals were not obtained in the condition in the absence of chloramphenicol or with chloramphenicol alone.

4.11 | Data collection and structure determination

X-ray data were collected at NE-CAT beamline 24-ID-C at Argonne National Laboratory. Data reduction was performed with the HKL2000 package (Otwinowski and Minor, 1997), and all subsequent data-processing steps were carried out using programs provided through SBGrid.[40] The crystals belong to space group $P2_12_12_1$ and diffracted to 1.35 Å. The structure of Chl-B2 was easily solved by molecular replacement using a VHH template (1BZQ) with all CDRs removed as the search model in Phaser_MR from the Phenix suite.[41] The asymmetric unit contains two Chl-B2 molecules. The missing CDR residues were added with automatic building routines. The

bound chloramphenicol was readily recognizable after the CDR residues were added. Iterative model building and refinement steps further improved the electron density maps and the model statistics. The C-terminal 14-residue affinity tag was not modeled, as spurious density indicates multiple alternate conformations. This led to a slightly higher R_{free} value of 23.4% than expected for a 1.35 Å structure. The stereochemical quality of the final model was validated by Molprobity.[42] Statistical parameters of data collection and refinement are all given in Table 3. Structure figures were created in PyMOL (Schrödinger LLC).

TABLE 3 X-ray data collection and refinement statistics for VHH Chl-B2

PDB code	Chl-B2 7TJC
Data collection	
Space group	$P2_12_12_1$
Cell dimensions	
a, b, c (Å)	43.2, 66.6, 93.2
Resolution (Å)	54.15–1.35 (1.40–1.35)[a]
$R_{p.i.m.}$ (%)	2.4 (39.8)
I/σ(I)	9.1 (1.0)
$CC_{1/2}$ (%)	99.9 (73.9)
Completeness (%)	99.7 (98.2)
Redundancy	12.7 (10.6)
Wilson B-factor (Å²)	13.9
Refinement	
Resolution (Å)	54.15–1.35 (1.40–1.35)
No. reflections	59,664
Reflections used for R_{free}	1997 (3.3%)
R_{work}/R_{free}	19.9/23.4
No. atoms	2,244
Protein	1937
Ligands	46
Solvent	261
B factors (Å²)	21.0
Protein	19.5
Ligands	25.4
Solvent, ions	35.6
Root mean squared deviations	
Bond lengths (Å)	0.006
Bond angles (°)	0.89
Ramachandran favored (%)	98.76
Ramachandran allowed (%)	1.24

[a]Values in parentheses for highest resolution shell.

AUTHOR CONTRIBUTIONS

Charles A. Swofford: Conceptualization (lead); data curation (lead); formal analysis (lead); investigation (lead); methodology (lead); validation (lead); visualization (lead); writing – original draft (lead); writing – review and editing (lead). **Sarah A. Nordeen:** Data curation (supporting); formal analysis (supporting); investigation (supporting); methodology (supporting); writing – review and editing (supporting). **Lu Chen:** Conceptualization (supporting); writing – review and editing (supporting). **Mahaam M. Desai:** Data curation (supporting). **Joanna Chen:** Data curation (supporting). **Stacy L. Springs:** Conceptualization (supporting); funding acquisition (equal); project administration (supporting); resources (equal); supervision (supporting); writing – review and editing (equal). **Thomas U. Schwartz:** Formal analysis (supporting); resources (supporting); supervision (supporting); visualization (supporting); writing – original draft (supporting); writing – review and editing (equal). **Anthony J. Sinskey:** Conceptualization (supporting); funding acquisition (equal); project administration (lead); resources (equal); supervision (lead); writing – review and editing (equal).

DATA AVAILABILITY STATEMENT

The data that support the findings of this study are available from the corresponding author upon reasonable request.

ORCID

Charles A. Swofford https://orcid.org/0000-0001-5885-8286
Stacy L. Springs https://orcid.org/0000-0003-2133-5689
Thomas U. Schwartz https://orcid.org/0000-0001-8012-1512
Anthony J. Sinskey https://orcid.org/0000-0002-1015-1270

REFERENCES

1. Office USGA Imported Seafood Safety: FDA and USDA Could Strengthen Efforts to Prevent Unsafe Drug Residues. 2017.
2. Anon Imported Seafood Safety: FDA Should Improve Monitoring of Its Warning Letter Process and Better Assess Its Effectiveness|U.S. GAO https://www.gao.gov/products/gao-21-231
3. Food and Water Watch A Decade of Dangerous Food Imports from China. 2011.
4. FDA Import Alert 16–131. 2019.
5. Liu YY, Wang Y, Walsh TR, et al. Emergence of plasmid-mediated colistin resistance mechanism MCR-1 in animals and human beings in China: A microbiological and molecular biological study. Lancet Infect Dis. 2016;16:161–168.
6. Luo Q, Wang Y, Xiao Y. Prevalence and transmission of mobilized colistin resistance (mcr) gene in bacteria common to animals and humans. Biosaf Health. 2020;2:71–78.
7. Shen C, Zhong LL, Yang Y, et al. Dynamics of mcr-1 prevalence and mcr-1-positive Escherichia coli after the cessation of colistin use as a feed additive for animals in China: A prospective cross-sectional and whole genome sequencing-based molecular epidemiological study. Lancet Microbe. 2020;1:e34–e43.
8. Dasenaki ME, Thomaidis NS. Multi-residue determination of seventeen sulfonamides and five tetracyclines in fish tissue using a multi-stage LC–ESI–MS/MS approach based on advanced mass spectrometric techniques. Anal Chim Acta. 2010;672:93–102.
9. Fedorova G, Nebesky V, Randak T, Grabic R. Simultaneous determination of 32 antibiotics in aquaculture products using LC-MS/MS. Chem Paper. 2014;68:29–36.
10. Li W, Shi Y, Gao L, Liu J, Cai Y. Investigation of antibiotics in mollusks from coastal waters in the Bohai Sea of China. Environ Pollut. 2012;162:56–62.
11. Serra-Compte A, Álvarez-Muñoz D, Rodríguez-Mozaz S, Barceló D. Multi-residue method for the determination of antibiotics and some of their metabolites in seafood. Food Chem Toxicol. 2017;104:3–13.
12. Cháfer-Pericás C, Maquieira Á, Puchades R. Fast screening methods to detect antibiotic residues in food samples. TrAC Trends Anal Chem. 2010;29:1038–1049.
13. Ingram JR, Schmidt FI, Ploegh HL. Exploiting Nanobodies' singular traits. Annu Rev Immunol. 2018;36:695–715.
14. Vincke C, Muyldermans S. Introduction to heavy chain antibodies and derived Nanobodies. Single domain antibodies. Totowa, NJ: Humana Press, 2012; p. 15–26.
15. Anderson GP, Liu JL, Hale ML, et al. Development of Antiricin single domain antibodies toward detection and therapeutic reagents. Anal Chem. 2008;80:9604–9611.
16. Alvarez-Rueda N, Behar G, Ferré V, et al. Generation of llama single-domain antibodies against methotrexate, a prototypical hapten. Mol Immunol. 2007;44:1680–1690.
17. Li D, Cui Y, Morisseau C, et al. Nanobody based immunoassay for human soluble epoxide hydrolase detection using polymeric horseradish peroxidase (PolyHRP) for signal enhancement: The rediscovery of PolyHRP? Anal Chem. 2017;89:6248–6256.
18. Ruth C. Ladenson, Dan L. Crimmins, Yvonne Landt and, Ladenson* JH (2006) Isolation and Characterization of a Thermally Stable Recombinant Anti-Caffeine Heavy-Chain Antibody Fragment.

19. Wang J, Bever CRS, Majkova Z, et al. Heterologous antigen selection of camelid heavy chain single domain antibodies against Tetrabromobisphenol a. Anal Chem. 2014;86:8296–8302.

20. He T, Wang Y, Li P, et al. Nanobody-based enzyme immunoassay for aflatoxin in agro-products with high tolerance to Cosolvent methanol. Anal Chem. 2014;86:8873–8880.

21. Tabares-Da Rosa S, Rossotti M, Carleiza C, et al. Competitive selection from single domain antibody libraries allows isolation of high-affinity antihapten antibodies that are not favored in the llama immune response. Anal Chem. 2011;83:7213–7220. https://doi.org/10.1021/ac201824z.

22. Kim HJ, McCoy MR, Majkova Z, et al. Isolation of alpaca antihapten heavy chain single domain antibodies for development of sensitive immunoassay. Anal Chem. 2012;84:1165–1171. https://pubmed.ncbi.nlm.nih.gov/22148739/.

23. Li D, Zang M, Li X, Zhang K, Zhang Z, Wang S. A study on the food fraud of national food safety and sample inspection of China. Food Control. 2020;116:107306.

24. Stadler RH, Verzegnassi L, Seefelder W, Racault L. Why semicarbazide (SEM) is not an appropriate marker for the usage of nitrofurazone on agricultural animals. Food Addit Contam Part A Chem Anal Control Expo Risk Assess. 2015;32:1842–1850.

25. Pírez-Schirmer M, Rossotti M, Badagian N, Leizagoyen C, Brena BM, González-Sapienza G. Comparison of three Anti-hapten VHH selection strategies for the development of highly sensitive immunoassays for microcystins. Anal Chem. 2017;89:6800–6806.

26. Spinelli S, Frenken LGJ, Hermans P, et al. Camelid heavy-chain variable domains provide efficient combining sites to Haptens†. Biochem Int. 2000;39:1217–1222. https://doi.org/10.1021/bi991830w.

27. Spinelli S, Tegoni M, Frenken L, van Vliet C, Cambillau C. Lateral recognition of a dye hapten by a llama VHH domain. J Mol Biol. 2001;311:123–129.

28. Fanning SW, Horn JR. An anti-hapten camelid antibody reveals a cryptic binding site with significant energetic contributions from a nonhypervariable loop. Protein Sci. 2011;20:1196–1207.

29. Tabares-da Rosa S, Wogulis LA, Wogulis MD, González-Sapienza G, Wilson DK. Structure and specificity of several triclocarban-binding single domain camelid antibody fragments. J Mol Recognit. 2019;32:e2755.

30. Ding L, Wang Z, Zhong P, et al. Structural insights into the mechanism of single domain VHH antibody binding to cortisol. FEBS Lett. 2019;593:1248–1256. https://doi.org/10.1002/1873-3468.13398.

31. Lesne J, Chang HJ, de Visch A, et al. Structural basis for chemically-induced homodimerization of a single domain antibody. Sci Report. 2019;9:1–4.

32. Bever CS, Dong JX, Vasylieva N, et al. VHH antibodies: emerging reagents for the analysis of environmental chemicals. Anal Bioanal Chem. 2016;408:5985–6002.

33. Moutel S, Bery N, Bernard V, et al. NaLi-H1: a universal synthetic library of humanized nanobodies providing highly functional antibodies and intrabodies. Elife. 2016;5:e16228.

34. McMahon C, Baier AS, Pascolutti R, et al. Yeast surface display platform for rapid discovery of conformationally selective nanobodies. Nat Struct Molecular Biology. 2018;25(3):289–296.

35. Yau KYF, Groves MAT, Li S, et al. Selection of hapten-specific single-domain antibodies from a non-immunized llama ribosome display library. J Immunol Method. 2003;281:161–175.

36. Doyle PJ, Arbabi-Ghahroudi M, Gaudette N, et al. Cloning, expression, and characterization of a single-domain antibody fragment with affinity for 15-acetyl-deoxynivalenol. Mol Immunol. 2008;45:3703–3713.

37. Ladenson J, Ladenson R, Landt Y, Crimmins D (2005) Methods for determining and lowering caffeine concentration in fluids.

38. Furst AL, Hoepker AC, Francis MB. Quantifying hormone disruptors with an engineered bacterial biosensor. ACS Cent Sci. 2017;3:110–116.

39. Truttmann MC, Wu Q, Stiegeler S, Duarte JN, Ingram J, Ploegh HL. HypE-specific Nanobodies as tools to modulate HypE-mediated target AMPylation. J Biol Chem. 2015;290:9087–9100.

40. Morin A, Eisenbraun B, Key J, et al. Cutting Edge: Collaboration gets the most out of software. Elife. 2013;2:e01456.

41. Liebschner D, Afonine P v, Baker ML, et al. Macromolecular structure determination using X-rays, neutrons and electrons: Recent developments in Phenix. Acta Crystallogr D Struct Biol. 2019;75:861–877. https://pubmed.ncbi.nlm.nih.gov/31588918/.

42. Chen VB, Arendall WB, Headd JJ, et al. MolProbity: All-atom structure validation for macromolecular crystallography. Acta Crystallogr D Biol Crystallogr. 2010;66:12–21. https://pubmed.ncbi.nlm.nih.gov/20057044/.

SUPPORTING INFORMATION

Additional supporting information can be found online in the Supporting Information section at the end of this article.